https://doi.org/10.5194/tc-2021-66
Preprint. Discussion started: 4 March 2021

The Cryosphere Discussions

Brief Communication: Thwaites Glacier cavity evolution

Suzanne L. Bevan[1], Adrian J. Luckman[1], Douglas I. Benn[2], Susheel Adusumilli[3], and Anna Crawford[2]

[1]Swansea University, Singleton Park, Swansea SA2 8PP
[2]University of St Andrews, College Gate, St Andrews KY16 9AJ
[3]Scripps Institution of Oceanography, University of California San Diego, La Jolla, CA, USA

Correspondence: Suzanne Bevan (s.l.bevan@swansea.ac.uk)

Abstract. Between 2014 and 2017, ocean melt eroded a large cavity beneath and along the western margin of the fast-flowing core of Thwaites Glacier. Here we show that from 2017 to the end of 2020 the cavity persisted but did not expand. This behaviour, of melt concentrated at the grounding line within confined sub-shelf cavities, fits with prior observations and modelling studies. We also show that acceleration and thinning of Thwaites Glacier grounded ice continue, with an increase in speed of 400 ma^{-1} and a thinning rate of 1.5 ma^{-1}, between 2012 and 2020.

1 Introduction

Much of the West Antarctic Ice Sheet (WAIS) is grounded below sea-level and exposed to oceanic warming at its periphery, making it a classic example of potential marine ice-sheet instability (Hughes, 1973; Schoof, 2007; Joughin et al., 2014). Any future collapse of WAIS is likely to be driven by retreat of its two largest outlet glaciers — Pine Island Glacier and Thwaites Glacier which together, by 2013, were discharging 258 Gta^{-1} of ice into the Amundsen Sea Embayment (ASE) (Mouginot et al., 2014). See Scambos et al. (2017), and references therein, for a thorough review of the particular importance of Thwaites Glacier within the WAIS system.

Recent observations indicate that the retreat of Thwaites Glacier is already underway with satellite and airborne altimetry showing up to 2 ma^{-1} of thinning over the lower reaches of the glacier (McMillan et al., 2014). From 2006, after 14 years of steady flow, the main trunk of Thwaites glacier began to accelerate. By 2013, velocity increases had lead to a 33% increase in ice flux across the grounding line with velocities increasing from 3 kma^{-1} to 4 kma^{-1} (Mouginot et al., 2014).

Dynamic change was accompanied by grounding line retreat. Beneath its central fast-flowing region the grounding line of Thwaites Glacier retreated inland down a retrograde bed slope by between 12 and 18 km between 1996 and 2011 (Rignot et al., 2014) (Fig. 1a). The grounding lines were mapped using differential interferometry applied to satellite-borne synthetic aperture radar (SAR) images and were updated by Milillo et al. (2019) using the same technique. Milillo et al. (2019) found that by 2016/2017 the grounding lines in many locations had further retreated. In particular, the grounding line parallel to, and west of the fast-flowing core had retreated by up to 3.2 km compared with 2011, migrating back and forth with the tidal cycle across a broad 2.5 km grounding zone.

Between 2011 and 2014, surface elevations of the ice in the area where the new grounding zone was to develop decreased by around 4 ma^{-1}. From mid-2014, as the ice went afloat and began to melt from below, thinning rates based on reductions in

https://doi.org/10.5194/tc-2021-66
Preprint. Discussion started: 4 March 2021


The Cryosphere Discussions
Open Access
EGU

hydrostatic thicknesses increased to 200 ma^{-1} (Milillo et al., 2019). By late 2016, a 350 m deep, 4×10 km cavity could be identified in radar depth soundings. Whilst the initial thinning was driven dynamically, the high melt rates within the new cavity were likely driven by the intrusion of warm modified Circumpolar Deep Water (mCDW) (Nakayama et al., 2019). The dense warm mCDW crosses the continental shelf and can access the ASE ice-shelf grounding lines via bathymetric troughs. Decadal variability in the flow of mCDW onto the continental shelf drives ASE ice-shelf thinning and glacier retreat on corresponding time-scales modified by local bed geometry (Jenkins et al., 2018).

In this study we use an extended time series of TanDEM-X digital elevation models (DEMs) and an updated bathymetry (Jordan et al., 2020) to examine the ongoing evolution of the new cavity. We also extend the record of wider area elevation change, and trends in surface velocities using TerraSAR-X and Sentinel-1 data.

2 Methods

2.1 TanDEM-X DEMs

We created a time series of 89 Digital Elevation Models from June 2011 to November 2020 based on experimental SAR data from the TanDEM-X satellite system. We used Gamma Remote Sensing software to interfere, unwrap, and phase scale (with the provided orbit vector data) the 2 m bistatic stripmap mode Co-registered Single look Slant range Complex images (CoSSCs). We initially geocoded the slant-range geometry DEMs to a horizontal resolution of 8 m using the RAMP DEM (Liu et al., 2015) gap-filled using the REMA DEM (Howat et al., 2019), then we iteratively refined the geocoding using the interferometrically generated DEM itself. The area is covered by two satellite scenes (Fig. 1a) mostly acquired on consecutive days (Appendix Table 1). We calibrated the southern most DEMs in the vertical using an ICESat-2 elevation acquired on 05 November 2018 located at a high-elevation slow-moving location (Fig. 1a). We tied the adjacent DEMs to their cotemporal neighbours using a point within the scene overlap. By choosing this point over a relatively flat region, height errors resulting from geolocation errors were minimised.

For elevations derived from ICESat-2 laser altimetry, we used data provided in the ATLAS/ICESat-2 L3A Land Ice Height (ATL06) product (Smith et al., 2020). We use the 'atl06_quality_summary' field to remove low-quality data due to high surface slope or roughness, high uncertainty in surface height, unreliable higher-level data, or cloudy conditions (Smith et al., 2019).

In order to map floating areas we adjusted the elevations from the WGS84 Ellipsoid datum to the EGM2008 Geoid (Pavlis et al., 2012) adding 1.81 m to allow for local mean dynamic topography (Armitage et al., 2018). We then assumed that any floating ice was in hydrostatic equilibrium to calculate a thickness (H) from the adjusted elevations (h) using Eq. 1 with an ice density (ρ_i) of 917 kgm^{-3}, seawater density (ρ_w) of 1028 kgm^{-3}, and a firn air depth f_a of 16 m. No tidal corrections were applied as maximum tidal ranges are small ($\pm$0.5 m).

$$H = \left((h - f_a) \times \frac{\rho_w}{\rho_w - \rho_i} \right) + f_a \quad (1)$$

https://doi.org/10.5194/tc-2021-66
Preprint. Discussion started: 4 March 2021

Where elevations minus hydrostatic thicknesses were above the bed depth (Jordan et al., 2020) the ice was assumed to be floating. The value for firn air depth can make a large difference to the floatation height. Using $f_a = 16$ m where the ice thickness is 800 m is equivalent to a mean ice density of 898 kgm^{-3}. Other studies that have attempted to correct ice density in Antarctic ice shelves either directly or via incorporating firn air depths have used values including 13–19 m of firn air (Griggs and Bamber, 2011) or 904 kgm^{-3} (Khazendar et al., 2016). We chose a value of 16 m following Jordan et al. (2020) who found that this value resulted in good agreement between grounding zones inferred from the REMA DEM, and interferometrically determined grounding zones (Rignot et al., 2014).

Orbit uncertainties (Krieger et al., 2013) mean that we cannot expect relative elevation accuracies across a scene better than 2 m. Nine of the TanDEM-X images since 2018 were acquired within 3 days of an ICESat-2 measurement located within their geographic coverage. Using only points that were measured on grounded ice, the mean difference between 24,030 collocated TanDEM-X and ICESat-2 elevations was 1.0 m (standard deviation 3.1 m). We therefore estimate an uncertainty in the TanDEM-X elevations of $\pm$3 m and in hydrostatic thickness of $\pm$26 m.

2.2 Ice surface velocities

We measured ice surface velocities by feature tracking pairs of both TerraSAR-X SLCs (2012–2014), and Sentinel-1A and B SLCs (2015–2020), using Gamma Remote Sensing software. TerraSAR-X is one of the pair of satellites in the TanDEM-X system and we present results obtained by tracking 23 SLC pairs over 11 days with image patches of approximately 1 km square, sampling every 40 m. Similarly, we present results based on the tracking of 558 pairs of Sentinel-1A and B data, over 6 or 12 days and sampling every 100 m. We filtered both sets of feature-tracked displacements: first by a signal to noise ratio based on the cross-correlation of image patches, and then according to deviation from the mean displacement within a neighbourhood. We converted the displacements from the SAR image geometry to ground range geometry, and geocoded the results using the RAMP/REMA DEM mosaic (Section 2.1).

3 Results

We get a good agreement in 2017 between the 2016/2017 interferometrically mapped grounding lines and our DEM derived ones (Fig. 1a). An exception is an area about 20 km west of Thwaites indicating either an underestimation of bedrock depth or a misinterpretation of interferometric fringe lines. Elevation changes of -50 to -60 m between 2014 and 2017 over the cavity location (Fig. 1b) confirm those presented by Milillo et al. (2019) (their Fig. S6). The ice here was inferred to have gone afloat during 2014 and basal melt rates were estimated to be up to 200 ma^{-1}.

Elevation changes between 2017 and 2020 (Fig. 1c) show that the earlier cavity erosion process has slowed but that the cavity has persisted, in other words only small changes in thickness have taken place. We extracted profiles of surface elevation and hydrostatic thickness along a flowline, based on the mean velocity direction, that passed through the area of maximum thickness change (Fig. 1a). Again, we get a good agreement between the 2016/2017 interferometric grounding lines and the locations where surface elevations at this time drop below floatation height. An exception is grounding line located at 112.5 km

https://doi.org/10.5194/tc-2021-66
Preprint. Discussion started: 4 March 2021

on Fig. 2a. High surface elevations indicate that it is very unlikely that ice here was floating even with tidal flexure, suggesting a possible error interpreting the fringe patterns in the Milillo et al. (2019) study. The profiles show that the ungrounding evolves spatially in the down-flow direction (Fig. 2b). As early as 2011 a small cavity apparently existed at 115 km along the flowline, we have no evidence that this cavity connected to the ocean until June 2013 suggesting that either bed or surface elevations are erroneously low here. A second cavity develops by April 2015, by which time we can identify a path to the ocean in a direction perpendicular to the flow. By June 2016 the cavities have merged and in January 2017 connect with the existing downstream ice shelf. Beyond 2017 and up to the end of 2020 the cavity remains fairly stable. The temporal evolution can be seen more easily in the supplementary movie.

The cross-flow profiles (Fig. 2b) show the cavity expanding steadily inland from 2011 to 2019 with a good agreement on grounding line locations in 2011 and 2016/2017 and confirming the >2 km grounding line migration zone after 2014. Our estimated cavity depths along both profiles are up to 200 m.

Thwaites Glacier and floating tongue continue to accelerate from 2012 to 2021. Over much of the fast flowing region speeds are 400 ma^{-1} greater in January 2021 than in January 2012 — an increase of more than 10% (Fig. A1a). Velocities at a point about 5–10 km upstream of the cavity location (Fig. 1c) are increasing at an average annual rate of 70 ma^{-1} with a maximum reached in mid 2020 (Fig. 3). Slowing since 2020 appears to be part of normal intra-annual variability. Thinning at this location is about 1.5 ma^{-1}.

4 Discussion

Our results show that the cavity beneath the newly floating region along the western border of Thwaites Glacier has not continued to expand beyond 2017. The stability of the grounding lines, which are now in regions of prograde bed slopes, indicates that the advection of ice here is matched by high thinning rates, either due to melt or dynamic thinning. Extremely high melt rates, up to 200 ma^{-1} (Milillo et al., 2019), were detected in the cavity between 2014 and 2017 and may now be maintaining the new grounding line positions. However, this melt has not resulted in a vastly increased cavity volume, a fact that is consistent with observations and model studies showing that high melt rates within shallow cavities are restricted to the vicinity of the grounding line. For example, new cavities exposed since 1993 beneath ASE ice shelves remain on average just 112 m thick with 95% of them less than 400 m thick; and the sub-shelf topography remains imprinted with the bed topography (Jordan et al., 2020).

Although coupled ice–ocean models (that compare well with observed retreat rates) show that thinning rates are initially high beneath newly ungrounded ice, after a couple of years the ocean circulation within the cavity adjusts, and melt and thinning become concentrated along the high basal slope regions close to the grounding line (Goldberg et al., 2012; Seroussi et al., 2017). On the same time-scale, melt close to the grounding line increases the local basal slope until the melt rate is balanced by advection of thicker ice. Once ocean circulation and basal slope have adjusted, the cavity geometry can remain stable. Without the ocean coupling, models that parameterise melt rate using, for example, a simple depth-dependent rate tend to overestimate the delivery of ocean heat and melt near the grounding line, and hence predict unrealistic grounding line retreat.

https://doi.org/10.5194/tc-2021-66
Preprint. Discussion started: 4 March 2021

The time-scales of the adjustment of ocean circulation and ice-base geometry may explain why the cavity beneath Thwaites Glacier expands for a few years and then maintains its shape. The fast flow of the ice and the locally restricted melting means that downstream cavity depth remains shallow.

In 2020, steadily increasing velocities and dynamic thinning of grounded ice continues beyond estimates published up to 2014, and although we measure thinning rates at the location plotted in Fig. 3 that are lower than the 4 ma^{-1} measured by Milillo et al. (2019) they are comparable with rates observed between 2009 and 2012 over the large areas of the glacier (McMillan et al., 2014). However, bed topography and ice-thickness close to floatation can superimpose rapid local change on the background long-term evolution of Thwaites and other WAIS glaciers in ASE. Although decadal-scale variability has been identified in ASE ocean circulation and in the volume of mCDW on the shelf (Jenkins et al., 2018), such variability is not necessary to generate transient change such as the observed sudden cavity expansion and subsequent stability. Coupled ocean–ice modelling also suggests that further ice-shelf thinning and acceleration of inland ice, where the bed slopes upwards inland, takes place over longer 10–100 year time-scales (Goldberg et al., 2012) so that further consequences of the 2011–2016 grounding-line retreat, here and elsewhere on Thwaites Glacier, may not have become apparent yet.

5 Conclusions

Using a time series of DEMs based on interferometric processing of TanDEM-X SAR images we have shown that the 2014–2017 grounding-line retreat and cavity development beneath the western flank of Thwaites Glacier persist with little change to the end of 2020. Based on existing model-based understanding we conclude that restricted ocean circulation within the cavity and concentration of melt at the grounding line are responsible for the maintenance of the cavity. On a wider-scale perspective, in 2020 acceleration and dynamic thinning of Thwaites Glacier continues at a similar rate beyond that already observed up to 2014.

Data availability. We will make the elevation profiles, and elevation and speed time series available on the NERC Polar Data Centre.

Video supplement. Please see Supplementary animation.

Author contributions. SB created and analysed the TanDEM-X DEMs, and drafted the manuscript. DB is principal investigator on the CALISMO project, AL produced the Sentinel-1 velocity data, and AS contributed the ICESat-2 data. All co-authors contributed to discussions on the text.

Competing interests. The authors declare that they have no conflicts of interest.

https://doi.org/10.5194/tc-2021-66
Preprint. Discussion started: 4 March 2021

Acknowledgements. The research was funded by Natural Environment Research Council (NERC) projects CALISMO (Calving laws for ice-sheet models, NE/P011365/1) and DOMINOS (Disintegration of marine ice-sheets using novel optimised solutions, NE/S006605/1). TanDEM-X data used for generating the DEMs surface velocities were supplied by DLR. Sentinel-1 data were supplied by the European Space Agency. The bed data were downloaded from the UK Polar Data Centre (https://ramadda.data.bas.ac.uk/repository/entry/show?entryid=7803de8b-8a74-466b-888e-e8c737bf21ce). Many thanks to Pietro Milillo, (Jet Propulsion Laboratory, California Institute of Technology, USA) for supplying the 2016/2017 grounding line locations.

https://doi.org/10.5194/tc-2021-66
Preprint. Discussion started: 4 March 2021

References

Armitage, T. W. K., Kwok, R., Thompson, A. F., and Cunningham, G.: Dynamic Topography and Sea Level Anomalies of the Southern Ocean: Variability and Teleconnections, Journal of Geophysical Research: Oceans, 123, 613–630, https://doi.org/https://doi.org/10.1002/2017JC013534, 2018.

Goldberg, D. N., Little, C. M., Sergienko, O. V., Gnanadesikan, A., Hallberg, R., and Oppenheimer, M.: Investigation of land ice-ocean interaction with a fully coupled ice-ocean model: 1. Model description and behavior, Journal of Geophysical Research: Earth Surface, 117, https://doi.org/https://doi.org/10.1029/2011JF002246, 2012.

Griggs, J. A. and Bamber, J. L.: Antarctic ice-shelf thickness from satellite radar altimetry, Journal of Glaciology, 57, 485–498, https://doi.org/10.3189/002214311796905659, 2011.

Howat, I. M., Porter, C., Smith, B. E., Noh, M.-J., and Morin, P.: The Reference Elevation Model of Antarctica, The Cryosphere, 13, 665–674, https://doi.org/https://doi.org/10.5194/tc-13-665-2019, 2019.

Hughes, T.: Is the west Antarctic Ice Sheet disintegrating?, Journal of Geophysical Research (1896-1977), 78, 7884–7910, https://doi.org/https://doi.org/10.1029/JC078i033p07884, 1973.

Jenkins, A., Shoosmith, D., Dutrieux, P., Jacobs, S., Kim, T. W., Lee, S. H., Ha, H. K., and Stammerjohn, S.: West Antarctic Ice Sheet retreat in the Amundsen Sea driven by decadal oceanic variability, Nature Geoscience, 11, 733–738, https://doi.org/10.1038/s41561-018-0207-4, 2018.

Jordan, T. A., Porter, D., Tinto, K., Millan, R., Muto, A., Hogan, K., Larter, R. D., Graham, A. G. C., and Paden, J. D.: New gravity-derived bathymetry for the Thwaites, Crosson, and Dotson ice shelves revealing two ice shelf populations, The Cryosphere, 14, 2869–2882, https://doi.org/https://doi.org/10.5194/tc-14-2869-2020, 2020.

Joughin, I., Smith, B. E., and Medley, B.: Marine Ice Sheet Collapse Potentially Under Way for the Thwaites Glacier Basin, West Antarctica, Science, 344, 735–738, https://doi.org/10.1126/science.1249055, 2014.

Khazendar, A., Rignot, E., Schroeder, D. M., Seroussi, H., Schodlok, M. P., Scheuchl, B., Mouginot, J., Sutterley, T. C., and Velicogna, I.: Rapid submarine ice melting in the grounding zones of ice shelves in West Antarctica, Nature Communications, 7, 13 243, https://doi.org/10.1038/ncomms13243, 2016.

Krieger, G., Zink, M., Bachmann, M., Bräutigam, B., Schulze, D., Martone, M., Rizzoli, P., Steinbrecher, U., Walter Antony, J., De Zan, F., Hajnsek, I., Papathanassiou, K., Kugler, F., Rodriguez Cassola, M., Younis, M., Baumgartner, S., López-Dekker, P., Prats, P., and Moreira, A.: TanDEM-X: A radar interferometer with two formation-flying satellites, Acta Astronautica, 89, 83–98, https://doi.org/10.1016/j.actaastro.2013.03.008, 2013.

Liu, H., Jezek, K. C., Li, L., and Zhao, Z.: Radarsat Antarctic Mapping Project Digital Elevation Model, Version 2., Boulder, Colorado USA. NASA National Snow and Ice Data Center Distributed Active Archive Center., https://doi.org/10.5067/8JKNEW6BFRVD, 2015.

McMillan, M., Shepherd, A., Sundal, A., Briggs, K., Muir, A., Ridout, A., Hogg, A., and Wingham, D.: Increased ice losses from Antarctica detected by CryoSat-2, Geophysical Research Letters, 41, 3899–3905, https://doi.org/https://doi.org/10.1002/2014GL060111, 2014.

Milillo, P., Rignot, E., Rizzoli, P., Scheuchl, B., Mouginot, J., Bueso-Bello, J., and Prats-Iraola, P.: Heterogeneous retreat and ice melt of Thwaites Glacier, West Antarctica, Science Advances, 5, https://doi.org/10.1126/sciadv.aau3433, 2019.

Mouginot, J., Rignot, E., and Scheuchl, B.: Sustained increase in ice discharge from the Amundsen Sea Embayment, West Antarctica, from 1973 to 2013, Geophysical Research Letters, 41, 1576–1584, https://doi.org/10.1002/2013GL059069, 2014.

https://doi.org/10.5194/tc-2021-66
Preprint. Discussion started: 4 March 2021

Nakayama, Y., Manucharyan, G., Zhang, H., Dutrieux, P., Torres, H. S., Klein, P., Seroussi, H., Schodlok, M., Rignot, E., and Menemenlis, D.: Pathways of ocean heat towards Pine Island and Thwaites grounding lines, Scientific Reports, 9, 16 649, https://doi.org/10.1038/s41598-019-53190-6, 2019.

Pavlis, N. K., Holmes, S. A., Kenyon, S. C., and Factor, J. K.: The development and evaluation of the Earth Gravitational Model 2008 (EGM2008), Journal of Geophysical Research: Solid Earth, 117, https://doi.org/https://doi.org/10.1029/2011JB008916, 2012.

Rignot, E., Mouginot, J., Morlighem, M., Seroussi, H., and Scheuchl, B.: Widespread, rapid grounding line retreat of Pine Island, Thwaites, Smith, and Kohler glaciers, West Antarctica, from 1992 to 2011, Geophysical Research Letters, 41, 3502–3509, https://doi.org/10.1002/2014GL060140, 2014.

Scambos, T. A., Bell, R. E., Alley, R. B., Anandakrishnan, S., Bromwich, D. H., Brunt, K., Christianson, K., Creyts, T., Das, S. B., DeConto, R., Dutrieux, P., Fricker, H. A., Holland, D., MacGregor, J., Medley, B., Nicolas, J. P., Pollard, D., Siegfried, M. R., Smith, A. M., Steig, E. J., Trusel, L. D., Vaughan, D. G., and Yager, P. L.: How much, how fast?: A science review and outlook for research on the instability of Antarctica's Thwaites Glacier in the 21st century, Global and Planetary Change, 153, 16–34, https://doi.org/10.1016/j.gloplacha.2017.04.008, 2017.

Schoof, C.: Ice sheet grounding line dynamics: Steady states, stability, and hysteresis, Journal of Geophysical Research: Earth Surface, 112, https://doi.org/https://doi.org/10.1029/2006JF000664, 2007.

Seroussi, H., Nakayama, Y., Larour, E., Menemenlis, D., Morlighem, M., Rignot, E., and Khazendar, A.: Continued retreat of Thwaites Glacier, West Antarctica, controlled by bed topography and ocean circulation, Geophysical Research Letters, 44, 6191–6199, https://doi.org/https://doi.org/10.1002/2017GL072910, 2017.

Smith, B., Fricker, H. A., Holschuh, N., Gardner, A. S., Adusumilli, S., Brunt, K. M., Csatho, B., Harbeck, K., Huth, A., Neumann, T., Nilsson, J., and Siegfried, M. R.: Land ice height-retrieval algorithm for NASA's ICESat-2 photon-counting laser altimeter, Remote Sensing of Environment, 233, 111 352, https://doi.org/10.1016/j.rse.2019.111352, 2019.

Smith, B., Fricker, H. A., Gardner, A., Siegfried, M. R., Adusumilli, S., Csathó, B. M., Holschuh, N., Nilsson, A., Paolo, F. S., and ICESat-2 Science Team: ATLAS/ICESat-2 L3A Land Ice Height, Version 3, Boulder, Colorado USA. NASA National Snow and Ice Data Center Distributed Active Archive Center., https://doi.org/10.5067/ATLAS/ATL06.003, 2020.

https://doi.org/10.5194/tc-2021-66
Preprint. Discussion started: 4 March 2021

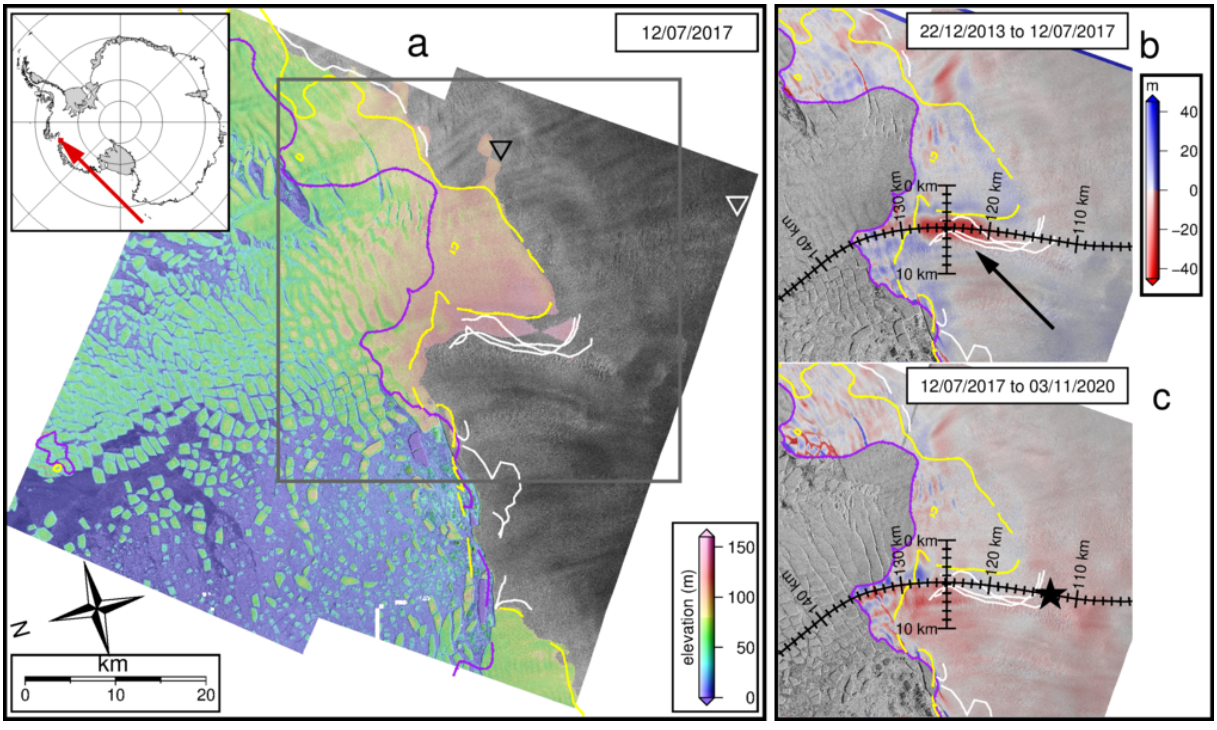

Figure 1. a) TanDEM-X elevations of floating areas for 12/07/2017. MEaSUREs grounding lines in purple (1996) and yellow (2011), Milillo et al. (2019) grounding lines in white. Black and white triangles mark the tie point locations for each DEM frame. Grey box shows the area covered by panels b and c. b) Elevation change based on TanDEM-X DEMs from 22/12/2013 to 12/07/2017. Profiles in black correspond to those plotted in Figs. 2a and b. The black arrow indicates the cavity referred to in the text. Grounding line colours as for panel a. c) As for b except elevation change is from 12/07/2017 to 03/11/2020. The black star marks the velocity extraction location for Fig. 3. Background shading on all panels is TerraSAR-X backscatter intensity.

https://doi.org/10.5194/tc-2021-66
Preprint. Discussion started: 4 March 2021

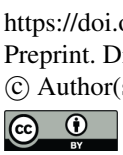

The Cryosphere
Discussions
Open Access
EGU

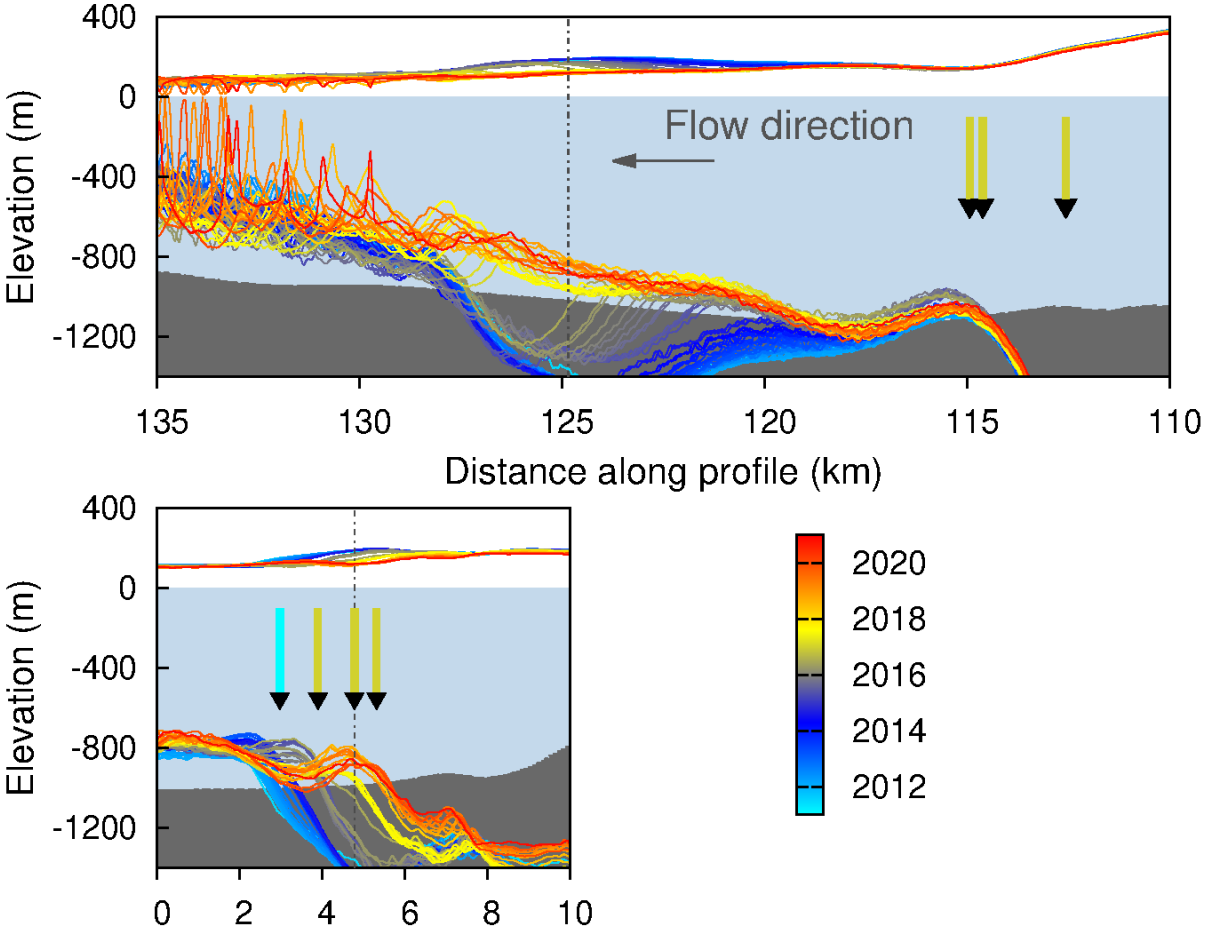

Figure 2. Ice surface elevation and hydrostatic thickness extracted from a) the along-flow profile, and b) the across-flow profile marked in Fig. 1b. Where the ice base assuming hydrostatic thickness lies below the bedrock elevation this should be interpreted as a scaled height-above-floatation where the scaling factor is $(\rho_w - \rho_i)/\rho_w$. Vertical dashed lines mark the intersections of the two profiles. Coloured arrows indicate grounding line locations for 2011 and 2016/2017 coloured according to year.

https://doi.org/10.5194/tc-2021-66
Preprint. Discussion started: 4 March 2021

The Cryosphere Discussions
Open Access
EGU

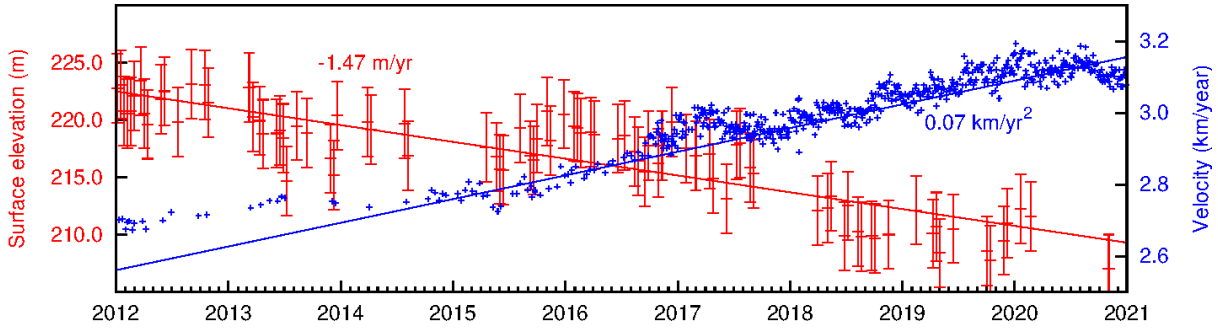

Figure 3. Time series of heights and surface speeds extracted at the point marked by the star in Fig. 1c. Vertical bars on the elevation points represent the ±3 m estimated error.

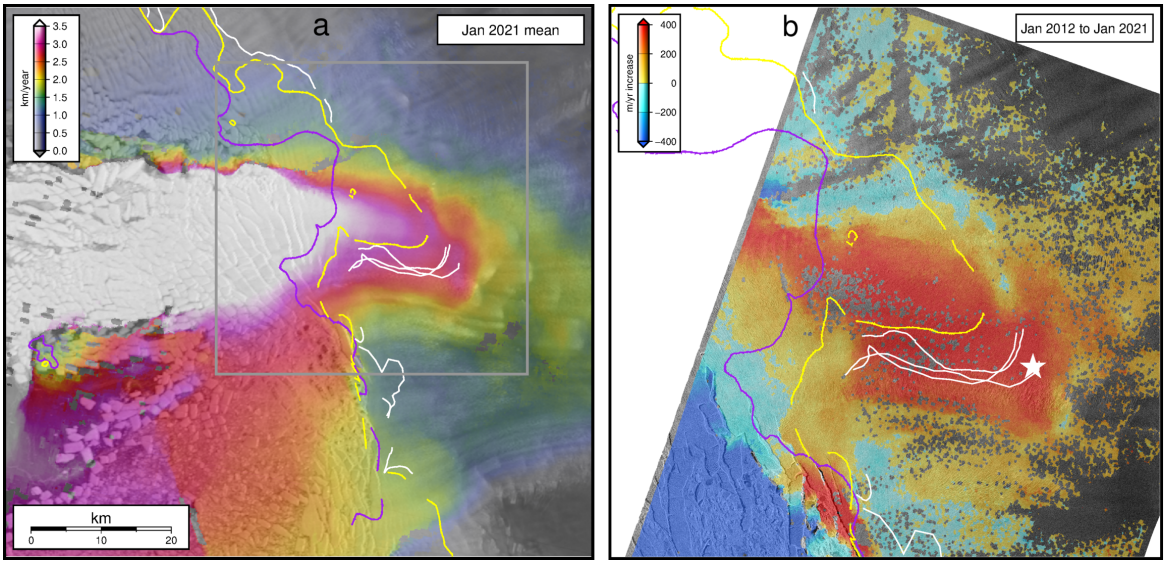

Figure A1. a) Mean surface speeds for January 2021 based on feature tracking Sentinel-1 data. b) Change in surface speed from January 2012 based on feature tracking TerraSAR-X data to January 2021 speeds. The white star marks the velocity extraction point.

https://doi.org/10.5194/tc-2021-66
Preprint. Discussion started: 4 March 2021


The Cryosphere Discussions
Open Access
EGU

Table A1. TanDEM-X DEM dates. Dates in bold indicate that adjacent scenes were not on consecutive dates.

North scene	South scene	East scene	West scene
07/01/2012	06/01/2012	20/04/2015	19/04/2015
18/01/2012	17/01/2012	23/05/2015	22/05/2015
29/01/2012	28/01/2012	03/06/2015	02/06/2015
09/02/2012	08/02/2012	14/06/2015	13/06/2015
20/02/2012	19/02/2012	10/09/2015	09/09/2015
02/03/2012	01/03/2012	21/09/2015	20/09/2015
24/03/2012	23/03/2012	04/11/2015	03/11/2015
04/04/2012	03/04/2012	15/11/2015	14/11/2015
15/04/2012	14/04/2012	29/12/2015	28/12/2015
29/05/2012	28/05/2012	11/02/2016	10/02/2016
09/06/2012	08/06/2012	22/60/2016	21/02/2016
23/07/2012	22/07/2012	26/03/2016	25/03/2016
05/09/2012	04/09/2012	06/04/2016	05/04/2016
19/10/2012	18/10/2012	22/06/2016	21/06/2016
30/10/2012	29/10/2012	28/01/2017	27/01/2017
11/03/2013	10/03/2013	02/03/2017	01/03/2017
22/03/2013	21/03/2013	15/04/2017	14/04/2017
13/04/2013	12/04/2013	**01/07/2017**	**08/06/2017**
24/04/2013	23/04/2013	12/07/2017	11/07/2017
07/06/2013	06/06/2013	23/07/2017	22/07/2017
18/06/2013	17/06/2013	05/09/2017	04/09/2017
29/06/2013	28/06/2013	02/04/2018	01/04/2018
10/07/2013	09/07/2013	10/07/2018	09/07/2018
12/08/2013	11/08/2013	**17/10/2018**	**05/10/2018**
14/09/2013	13/09/2013	19/11/2018	18/11/2018
30/11/2013	29/11/2013	15/02/2019	14/02/2019
11/12/2013	10/12/2013	22/04/2019	21/04/2019
22/12/2013	21/12/2013	03/05/2019	02/05/2019
09/03/2014	08/03/2014	16/06/2019	15/06/2019
31/03/2014	30/03/2014	**17/11/2019**	**27/11/2019**
11/04/2014	10/04/2014	**11/01/2020**	**21/01/2020**
30/07/2014	29/07/2014	22/01/2020	21/01/2020
10/08/2014	09/08/2014	03/11/2020	02/11/2020